p-ISSN 2301–4156 | e-ISSN 2460–5719

Performance Comparison of Generalized Frequency Division Multiplexing Using QAM and OQAM

Ari Endang Jayati[1], Budiani Destyningtias[2]

[1,2] Electrical Engineering Department, Faculty of Engineering Universitas Semarang, Jl. Soekarno Hatta Semarang 50196 INDONESIA (tel.: 024-6702757; fax: 024-67022722; email: [1]ariendang@usm.ac.id; [2]destyningtias@usm.ac.id

[Received: 21 January 2022, Revised: 25 November 2022]
Corresponding Author: Ari Endang Jayati

ABSTRACT — Generalized frequency division multiplexing (GFDM) is a future nonorthogonal multicarrier system. GFDM is a block-shaped data transmission technique in which each subcarrier is formed from nonrectangular shaped pulses. The application of quadrature amplitude modulation (QAM) mapping for GFDM is excellent because of the increased spectral efficiency. QAM also has limitations, namely increasing complexity when implemented. Apart from that, the inter carrier interference (ICI) persists and greatly influences the system. The technique for mitigating this weakness is by using offset QAM (OQAM) mapping. The advantages of GFDM/OQAM over GFDM/QAM are that the quadrature and in-phase components in OQAM modulation do not experience shifts in the same time slot, low out of band (OOB), high data rate and is ICI free. This study compares two scenarios namely the GFDM/OQAM and the GFDM/QAM systems. It analyzes the performance of the bit error rate (BER) if additive white gaussian noise (AWGN) and Rayleigh channels are passed. The simulation results show that GFDM/OQAM has better performance results. The simulation results showed that in order to obtain BER 10^{-2}, there should be a decrease in the value of E_b/N_0 (ratio of energy per bit to noise power) by 8 dB in QAM to OQAM when they were passed AWGN channels. Meanwhile, when passed the Rayleigh Fading channel, there was a decrease in the E_b/N_0 value by 9 dB in the QAM to OQAM to get a BER value of 10^{-2}. This study has also succeeded in investigating the performance of the two systems for parameters of the constellation diagram and signal spectrum. Moreover, it has succeeded in obtaining a roll off factor reference value that can be used in the application of the GFDM/OQAM system with the best performance result of 0.3. The roll off factor value greatly affects the performance of the GFDM system.

KEYWORDS — GFDM, ICI, Nonorthogonal, OQAM, QAM.

I. INTRODUCTION

Future wireless communication technology applications require a high spectrum efficiency, fast data rate, and low complexity. Examples of these applications include machine to machine (M2M) and internet of things (IoT) applications. Currently, the multicarrier technique applied is orthogonal frequency division multiplexing (OFDM). OFDM has several drawbacks, including the out of band (OOB) and high peak average power ratio (PAPR). High OOB and PAPR values will result in truncation of the input signal so that the information signal is distorted. Due to these limitations, it is necessary to research other multicarrier candidates that meet the requirements of these future applications.

To overcome this problem, a GFDM multicarrier system is proposed. GFDM is a nonorthogonal filtered-multicarrier system in which each subcarrier is formed from nonrectangular shaped pulses. GFDM is based on block independent modulation, with each block divided into subsymbols and subcarriers. Each subcarrier is filtered with a circularly shifted prototype filter in the frequency domain and time domain [1].

Common GFDM uses quadrature amplitude modulation (QAM). The QAM will increase the efficiency of the signal spectrum. However, QAM also has limitations, namely there is still inter-carrier interference (ICI) and the high complexity of its implementation [2]. The method of mitigating these limitations is by using offset QAM (OQAM) mapping. In the QAM, there is a phase jump of 180º; while in the OQAM, there is a phase shift of 90º. The quadrature and in-phase components in the OQAM do not experience a shift in the same time slot. Therefore, the phase shift is never greater than 90º. Even though the signal spectrum overlaps, it does not cause crosstalk between subcarriers on adjacent channels for OQAM mapping. It is due to the half-time symbol delay between the quadrature and in-phase components on the subcarrier [3]. In addition, the system will also minimize the ICI effect by reducing the distance between adjacent channels for each subcarrier. The application of OQAM mapping to the GFDM system is better than QAM. The benefits of GFDM/OQAM can meet application requirements with high data rates and ICI-free.

Little research has been done on OQAM in GFDM. The application of GFDM/OQAM to the Rician and Rayleigh channels has been carried out [3]-[12]. The application of GFDM in various fields has also been studied [13]-[18]. However, these studies have not yet discussed the analysis of system performance on Rayleigh channels. In addition, only a few parameters were studied. The contribution of this study is to compare the performance of GFDM/QAM with GFDM/OQAM through the AWGN and Rayleigh channels. Based on the existing literature, there have been no articles on the performance of GFDM on both systems in national journals. Therefore, it is essential to conduct this study. The next contribution is to compare the performance of the two systems for the BER parameters, constellation diagrams, and signal spectrums. In addition, the effect of the roll off factor (α) on the performance of GFDM was observed.

The organization of this paper is as follows: the second part discusses the GFDM/QAM and GFDM/OQAM models, the third part discusses the decrease in the BER formula that is passed on the AWGN and Rayleigh channels. The results and discussion are presented in the fourth section, while the fifth section presents the conclusion.

II. SYSTEM MODEL

GFDM is a multi-carrier system using flexible pulse shaping. GFDM is a candidate for future waveforms that use OFDM, but the GFDM output is obtained by summing multiple

p-ISSN 2301–4156 | e-ISSN 2460–5719

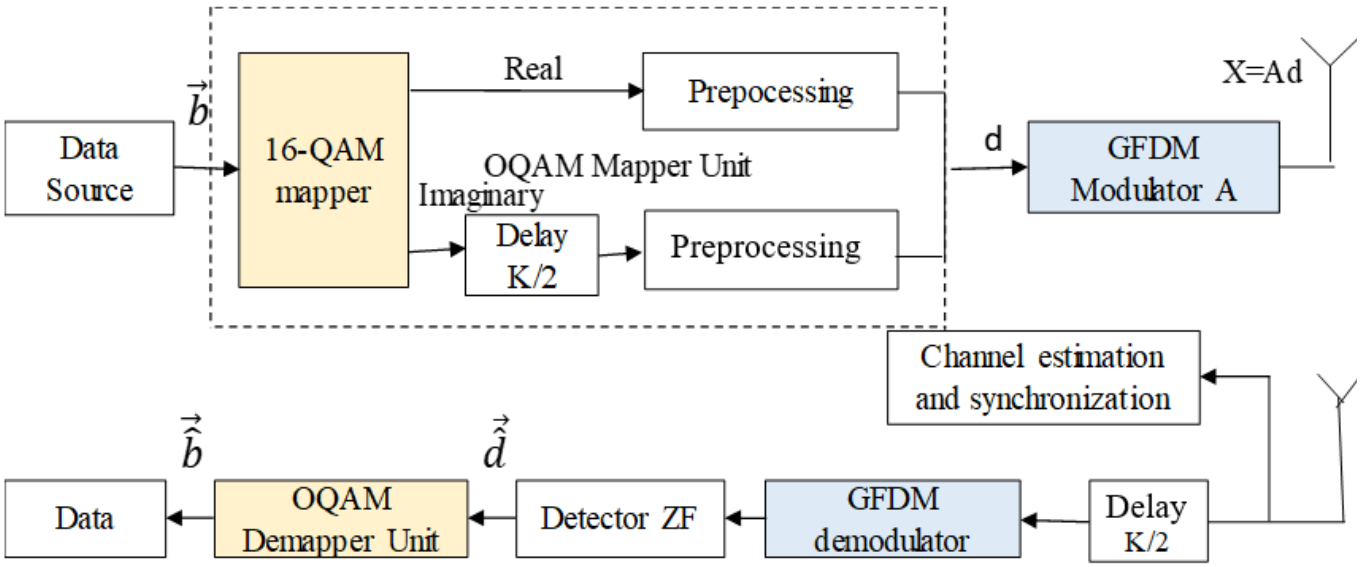

Figure 1. Block diagram of GFDM/OQAM.

data carrier signals with specific subcarriers and subsymbols. GFDM is a block-shaped modulation system, which consists of several subsymbols and subcarriers. Each subcarrier is filtered by a prototype filter that shifts circularly in the frequency and time domains. This technique can reduce OOB, increase spectrum efficiency and minimize intersymbol interference (ISI) and ICI [1].

GFDM has a low OOB so that it can overcome the weaknesses of OFDM. This is because GFDM is affected by the application of a pulse shaping filter on each subcarrier. GFDM also has a cyclic prefix (CP) to minimize ISI when passed on a multipath channel. The simple structure of GFDM makes synchronization easier and can reduce the energy use [19].

Figure 1 is the block diagram of the GFDM/OQAM system. The input information signal is a binary data series $\vec{b}$ converted to code data $\vec{b}_c$. The data were then mapped into a mapper block into a row of symbols. Mappers applied were QAM and OQAM. M-ary QAM has M different combinations of data bits of *n*. The outputs of the QAM and OQAM mappings are called vector data $\vec{d}$, which can also be described as $\vec{d} = d_0, d_1, \ldots, d_{N-1}$ with *N* is the sum of all symbols. Then, the vector data were changed to small speed data and would be decomposed into GFDM measuring *KxM*, with variable *K* is the number of subcarriers and *M* is the subsymbol in GFDM [7]. Hence, the result vector of the process can be represented as $\vec{d} = d_{0,0}, d_{1,0}, \ldots, d_{K-1,M-1}$.

The components of GFDM/OQAM are similar to those in GFDM/QAM, however, they have slight differences. The difference is the sample shift between in-phase and quadrature components of K/2 on complex data in the time domain for QAM mapping. A good OQAM mapper can reduce ICI/ISI efficiency.

The use of complex baseband data symbols in the GFDM/QAM system is a real data symbol modulated by OQAM sent to each subcarrier with a synthesis of the basis function derived from the time-frequency version of the prototype function with (1) [4].

$$g_{k,m}(n) = g\left[\left(n - \frac{mK}{2}\right) mod\ KM\right] e^{\frac{j2\pi k}{K}\left[n - \frac{L_p - 1}{2}\right]} \quad (1)$$

where $n = 0, 1, \ldots KM - 1$, $g_{k.m}(n)$ is a prototype function $g(n)$ which is circularly shifted in the frequency and time domains. The complex exponential form uses a phase component that has a delay and also undergoes rotational operations. Lp is the length of the prototype function. The superposition process for the data sent is in the form of discrete time. The GFDM/OQAM output can be presented in (2) [20].

$$x(n) = \sum_{k=0}^{K-1} \sum_{m=0}^{M-1} a_k(m) g_{k,m}(n) e^{j\phi m,k}. \quad (2)$$

where $n = 0, 1, \ldots KM - 1$, a_k(m) is data in the form of complex output of QAM mapping and $\emptyset_{m,k} = \frac{(k+m)\pi}{2}$, $e^{j\emptyset_{m,k}}$ shows a phase difference of π/2 between data a_k(m).

The signal received at the receiver side after being exposed to propagation through the wireless channel can be written in (3) [1].

$$r = Hx + w\,. \quad (3)$$

where $\boldsymbol{H} = circ\{\hat{h}\}$ is circular convolution channel matrix; $\hat{h}$ is zero padding from *h*, which is similar to *x*; $w \sim \mathcal{CN}(0, \sigma_w^2 I_{KM})$ is AWGN noise with different variances σ_w^2; and I_{KM} is an identity matrix with order *KM*. Form *r*(*n*) can be written down as $r(n) = x(n) * h(n) + w(n)$, where $*$ is a convolution process and *h*(*n*) is an impulse response in the fading channel. The AWGN channel matrix is written *h*(*n*) = 1, which is the same as **H** = **I**.

The first step on the receiver side was to remove the CP that had been added to the transmitter. As a result, only the actual information symbols remained. After the CP was removed, the fast Fourier transform (FFT) was carried out to convert the time domain data into a frequency domain and separate the information signal from the carrier signal. This process is a demodulation process and is the opposite of the inverse fast Fourier transform (IFFT). The demodulator process in 16-QAM is the reverse process of the 16-QAM modulator. The demodulator process on 16-QAM aims to convert the GFDM symbol sequence back into the original data bits sent [7]. The BER value is the ratio of the bit error received at the receiver side compared to the initial information bit at the transmitter. In this study, the method used was zero forcing (ZF) which is shown in (4). The trick is to create an identity matrix I and form

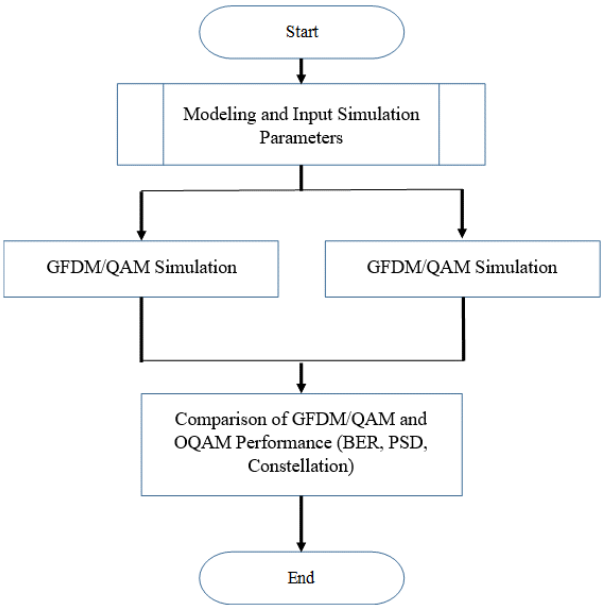

Figure 2. Research flowchart.

a matrix $\mathbf{A}^+$, where $\mathbf{A}^+\mathbf{A} = \mathbf{I}$. Matrix $\mathbf{A}^+ = (\mathbf{A}^H\mathbf{A})^{-1}\mathbf{A}^H$ can be denoted as $\mathbf{A}^+ = \mathbf{A}^H(\mathbf{A}\mathbf{A}^H)^{-1}$ [1].

$$d_{ZF} = \boldsymbol{A}^+ y. \quad (4)$$

III. PERMORMANCE ANALYSIS

In this section, the performance analysis of the two systems will be discussed. The flow chart of this research can be seen in Figure 2. The mathematical form of the 16-QAM signal is represented in (5).

$$S(t) = \sqrt{\frac{2E_{min}}{T_s}} I(t)\, cos[2\pi f_o t] - \sqrt{\frac{2E_{min}}{T_s}} Q(t)\, sin[2\pi f_o t] \quad (5)$$

where E_{min} is the signal energy that has the lowest amplitude and a_i, b_i is an integer chosen according to the position of the signal. Score $I(t)$ is ± 1 and $Q(t)$ is ± 3. $I(t)$ and $Q(t)$ are elements of a matrix of size LxL. The values of $I(t)$ and $Q(t)$ are shown in (6), with the value $L = \sqrt{M}$, for 16-QAM modulation (M = 16, L = 4).

$$(I(t), Q(t)) = \begin{bmatrix} (-3,3) & (-1,3) & (1,3) & (3,3) \\ (-3,1) & (-1,1) & (1,1) & (3,1) \\ (-3,3) & (-1,-1) & (1,-1) & (3,-1) \\ (-3,-3) & (-1,-3) & (1,-3) & (3,-3) \end{bmatrix} \quad (6)$$

In this section, the performance of QAM and GFDM/OQAM will be analyzed analytically. On the flat fading channel, the noise enhancement factor (NER) value is shown in (7) [2]

$$\zeta = \sum_{n=0}^{KM-1} \left| [d_{ZF}]_{k,n} \right|^2. \quad (7)$$

where ζ the same for all k values.

The value of SER GFDM/OQAM for the AWGN channel is denoted in (8) [2].

$$p_{AWGN}(e) = 2\left(\frac{k-1}{k}\right) erfc(\sqrt{\gamma}) - \left(\frac{k-1}{k}\right) erfc^2(\sqrt{\gamma}) \quad (8)$$

TABLE I
PARAMETER SIMULATION

Parameter	Notation	GFDM
Subcarrier	K	5
Subsymbols	M	9
Pulse shaping	g	Root raised cosine
Roll of factor	α	0;0.3;0.5;1
Mapping		16 QAM dan 16 OQAM

The GFDM/OQAM SNR system has the form as (9) and (10)

$$\gamma = \frac{3R_T}{2(2^{\mu}-1)} \cdot \frac{N_s E_s}{\zeta N_o} \quad (9)$$

and

$$R_T = \frac{KM}{KM+N_{CP}+N_{CS}}. \quad (10)$$

where μ is the number of bits per symbol QAM, $k = \sqrt{2^{\mu}}$, N_{CP} is the length of the cyclic prefix and cyclic suffix N_{CS}, K and M represents the number of subcarriers and subsymbols, E_s is the average energy per symbol and N_o is the noise power density. The N_s factor has a value of 2 for OQAM and 1 for QAM.

The SER GFDM/OQAM value for the Rayleigh channel is written in (11) [2]

$$p_{RAY}(e) = 2\left(\frac{p-1}{p}\right)\left(1 - \sqrt{\frac{\bar{\gamma}_r}{1+\bar{\gamma}_r}}\right) - \left(\frac{p-1}{p}\right)^2 \left[1 - \frac{4}{\pi}\sqrt{\frac{\bar{\gamma}_r}{1+\bar{\gamma}_r}} arctan\left(\sqrt{\frac{1+\bar{\gamma}_r}{\bar{\gamma}_r}}\right)\right] \quad (11)$$

where $\bar{\gamma}_r$ is the SNR in the Rayleigh channel; $\bar{\gamma}_r = \frac{3R_T\sigma_r^2}{(2^{\mu}-1)} \cdot \frac{N_s E_s}{\zeta N_o}$ and $\sigma_{ray}^2 = \sigma_r^2 \sum_{j=0}^{N_{ch}-1} |h_j|^2$. h is the impulse response of the channel with length Nch and σ_r^2=1/2 Rayleigh tap parameters distributed based on the SER performance.

IV. RESULT AND DISCUSSION

This section presents the results of investigations using simulations on the GFDM/OQAM and QAM systems. The comparison of the performance of the GFDM/OQAM and GFDM/QAM systems can be analyzed after the successful running of the program. The simulation used MATLAB R2015a. This study was conducted using the modeling of Figure 1, namely the GFDM/QAM and OQAM systems. In this simulation, the parameters used were in accordance with Table I.

A. GFDM/QAM SIMULATION RESULTS ON THE AWGN CHANNEL

The GFDM/QAM was simulated with variations in the Roll-of-factor (α) value of 0.3, 0.5, and 1, when passed on the AWGN channel. The comparison of BER on GFDM/QAM with variation of α is shown in Figure 3. The simulation results of the GFDM/QAM system for a value of α = 0.3 showed that a system with E_b/N_0 10 dB had a BER performance of 0.025. Whereas, the GFDM/QAM system of α = 0.5 produced a BER of 0.035, and for α=1 produced BER of 0.07.

The GFDM/QAM system with the best performance results used a value of α = 0.3, while the value of α = 1 achieved the lowest system performance. The selection of the pulse shaping

JURNAL NASIONAL TEKNIK ELEKTRO DAN TEKNOLOGI INFORMASI
p-ISSN 2301–4156 | e-ISSN 2460–5719

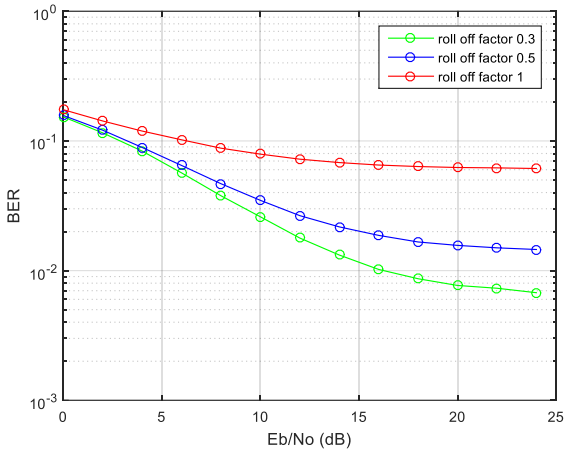

Figure 3. Comparison of BER on OFDM/QAM over AWGN channel.

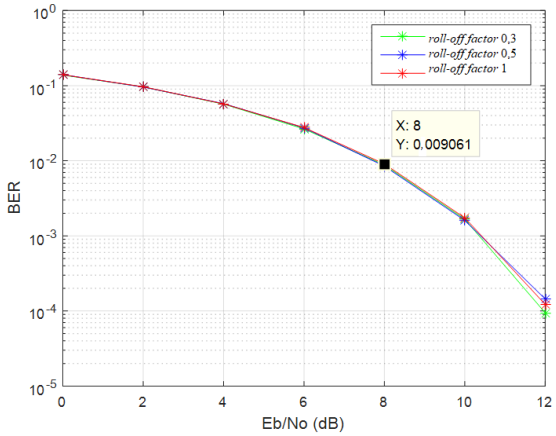

Figure 4. OFDM/OQAM BER graphs are passed through the AWGN channel.

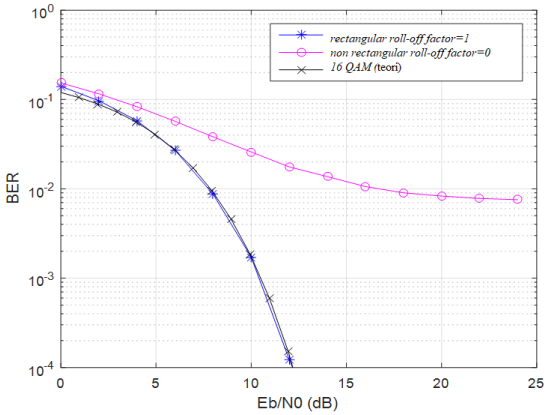

Figure 5. Comparison OFDM/QAM system with rectangular and nonrectangular pulse shaping.

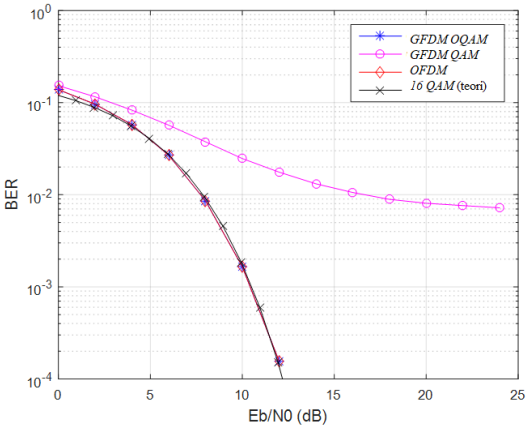

Figure 6. Comparison of BER OFDM/OQAM and QAMA over AWGN channel (α=0.3).

value on the GFDM/QAM is the reason for this. Based on the results in Figure 3, the greater the value of α or close to 1, the higher the BER value, meaning that the system performance is decreasing. The cause was the spectrum overlap between subcarriers. The overlap between these subcarriers produced interference which affected the magnitude of the error value at the receiver, resulting in a greater BER value.

B. GFDM/OQAM SIMULATION RESULTS ON AWGN CHANNELS

Similar to the previous simulation, in this section the BER on the GFDM/OQAM system passed on the AWGN channel is presented in Figure 4 with value variations of 0.3; 0.5; and 1. In this simulation, a comparison curve between GFDM/QAM, GFDM/OQAM, OFDM, and 16 QAM (theory) was created, as shown in Figure 5.

The simulation of the GFDM/OQAM system with value variations of 0.3; 0.5; and 1 yielded almost the same BER curve. In contrast to the performance of GFDM/QAM, the performance of the GFDM/OQAM system for all values of had better performance. For example, to obtain a BER value of 10^{-3}, an E_b/N_0 value of 11dB was required. Therefore, it can be concluded that the selection of the value of greater than 0 on the GFDM/OQAM results in better performance.

C. COMPARISON OF BER GFDM/QAM WITH RECTANGULAR AND NONRECTANGULAR PULSE SHAPING ON AWGN

The modeling parameters used in this section are still the same as the previous parameters. In this section, the GFDM/QAM system with values varying from 0 and 1 is investigated. The value of α = 0 indicate a rectangular or square-shaped pulse shaping, while the value of α = 1 is pulse shaping in the form of nonrectangular or not square. BER performance of the GFDM/QAM system is obtained from the comparison of the two roll-of-factor values. The value of BER against E_b/N_0 is presented in Figure 5.

Based on Figure 5, it can be seen that the use of rectangular pulses in the GFDM/QAM system with a value of E_b/N_0 10 dB has a BER performance of 0.0016. Meanwhile, the use of pulse shaping in the form of a nonrectangular pulse resulted in the performance of 0.0249. This simulation suggests that BER performance in GFDM/QAM with rectangular pulse shaping is better than GFDM/QAM which uses nonrectangular pulse shaping.

In this study, it can be seen that the performance of BER in GFDM/QAM with rectangular pulse shaping is better than the nonrectangular GFDM/QAM system. The BER value decreased to 99.99% at E_b/N_0 of 15 dB. When the GFDM/QAM system with pulse shaping was in the form of root raised cosine or nonrectangular, the output signal lost its orthogonality. In order to achieve better BER performance, the system should use α = 0 or rectangular. It is crucial to maintain the signal orthogonality so as to avoid interference between subcarriers.

D. COMPARISON OF BER GFDM/OQAM PULSE SHAPING RECTANGULAR AND NON-RECTANGULAR ON AWGN

In the previous section, the performance of BER when passing AWGN channels with different modulations based on the selection of roll-of-factor values has been observed. An investigation was carried out through simulation of the GFDM/OQAM system compared to GFDM/QAM with a value

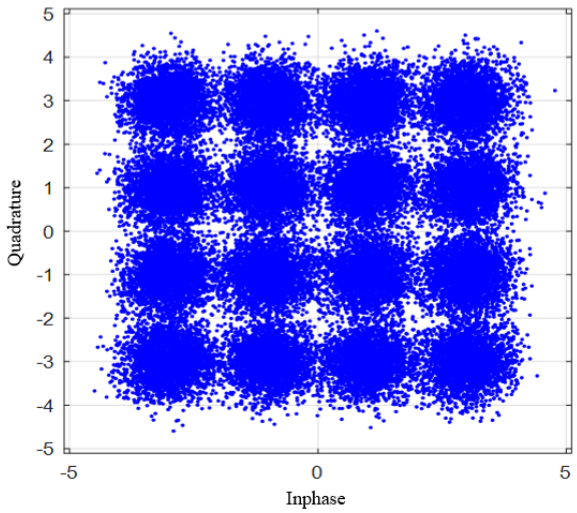

Figure 7. Scatterplot of OFDM/QAM systems.

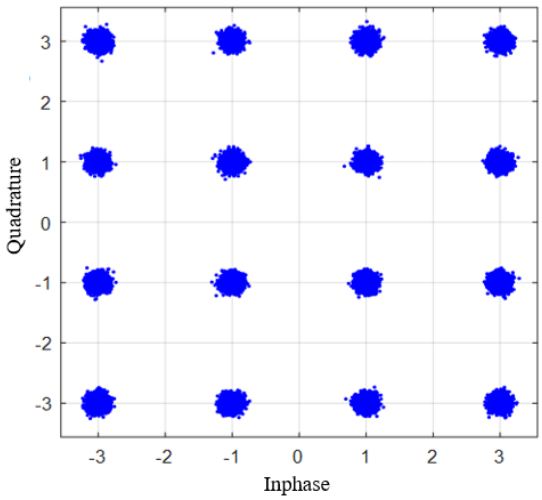

Figure 8. Scatterplot OFDM/OQAM systems.

of 0.3. The BER performance of both GFDM systems was then obtained. The BER and E_b/N_0 values of the GFDM system using the value α = 0.3 can be shown in Figure 6.

Based on Figure 6, it can be seen that the BER curve of GFDM/OQAM is better than that of GFDM/QAM. To obtain a BER value of 0.0013, a value of E_b/N_0 10 dB is required for the GFDM/OQAM system. Meanwhile, the GFDM/QAM system has a BER value of 0.024 for the same E_b/N_0 value. Hence, the BER performance of the GFDM/OQAM system is better than that of GFDM/QAM for the value of α = 0.3. The magnitude of the value of E_b/N_0 affects the GFDM system, namely the greater the value of E_b/N_0, the smaller the BER value obtained. If the noise power is greater, the value of E_b/N_0 will be smaller which will cause more and more bits to be received to be wrong.

Hence, it can be concluded that the performance of BER GFDM/OQAM is better than BER GFDM/QAM. The reduction of BER from GFDM/QAM to GFDM/OQAM can be up to 99.96% for the value of E_b/N_0 15dB [7].

Scatter plots of simulation results from GFDM/OQAM and GFDM/QAM are shown in Figure 7 and Figure 8. Scatter plots or constellation diagrams are useful for knowing the symbol detection area on the receiving side of the GFDM system.

The constellation diagrams for symbols in the GFDM/OQAM system are seen close to each other. These symbols are in the decision area. Meanwhile, the constellation diagram on GFDM/QAM shows that the symbol spreads at all

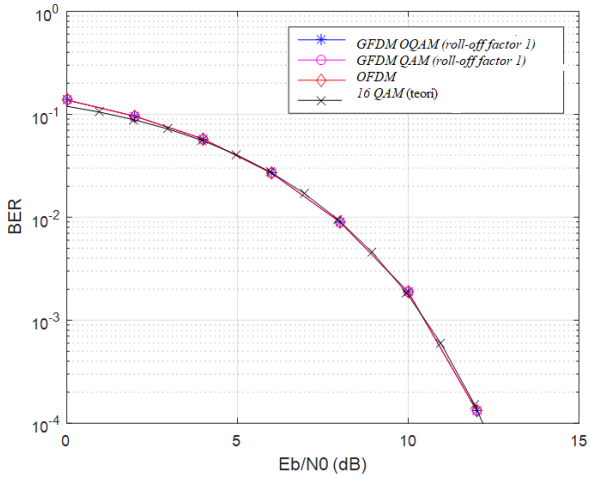

Figure 9. BER on OFDM/OQAM (α=1) and COFDM/QAM (α=0).

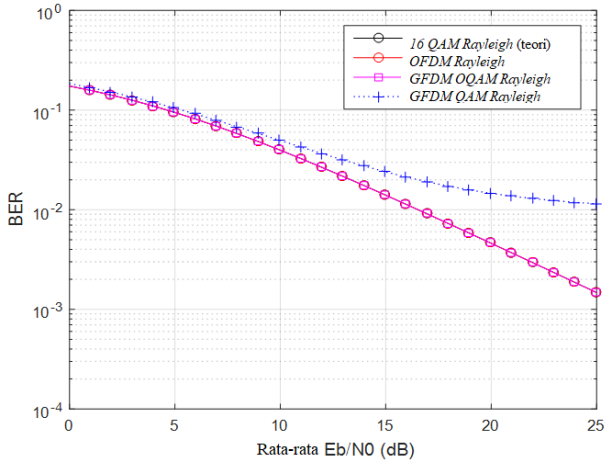

Figure 10. Comparison of BER OFDM/QAM and OFDM/QAM on Rayleigh channel for α = 1.

points and falls off the symbol detection region at the receiver. The result is that the BER value is not 0.

E. COMPARISON OF GFDM/OQAM AND GFDM/QAM VARIOUS A ON AWGN CHANNELS

This section will investigate the performance of GFDM/QAM and GFDM/OQAM using varying values of α = 0 on QAM and α = 1 on OQAM. The value of α = 0 means using a rectangular shaped pulse shaping. While the value of α = 1 means using nonrectangular pulse shaping. The BER obtained by the two different values of α or pulse shaping was then compared for its performance. The BER simulation results for E_b/N_0 for both systems can be seen in Figure 8.

Figure 9 shows that the GFDM/QAM system with rectangular pulse shaping and GFDM/OQAM with nonrectangular pulse shaping have relatively same E_b/N_0 values. Value obtained BER 10^{-2} for GFDM/OQAM and QAM required E_b/N_0 of 8 dB. Therefore, it can be seen that when using nonrectangular shaped pulse shaping, OQAM mapping must be used so that it does not cause interference between subcarriers so that orthogonality can be maintained. The BER performance of the GFDM/QAM system using rectangular pulse shaping was as good as that of the nonrectangular GFDM/OQAM.

F. COMPARISON OF GFDM/OQAM AND QAM VIA RAYLEIGH FADING CHANNEL

After the simulation to obtain the BER performance of the GFDM system on the AWGN channel, the next step is the

p-ISSN 2301–4156 | e-ISSN 2460–5719

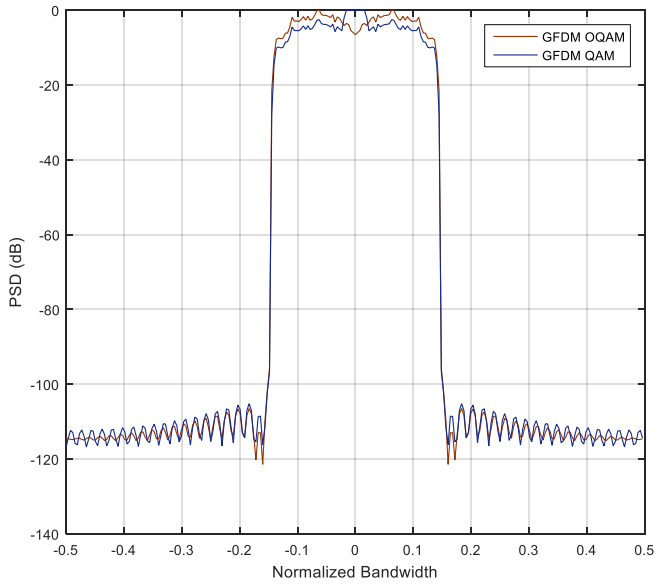

Figure 11. PSD on OFDM/OQAM and GFDM/QAM systems.

simulation to obtain the BER performance of the Rayleigh Fading channel. Similar to the previous simulation on the AWGN channel, the GFDM/OQAM and QAM systems were simulated using a variation of the value of α, namely 0.3, 0.5, and 1. The subsequent step is comparing the performance of the BER obtained in the two scenarios. The simulation results of BER against E_b/N_0 in GFDM with a value of $\alpha = 1$ are shown in Figure 10.

Figure 10 shows that the BER value of GFDM/OQAM is better than that of GFDM/QAM. When the value of E_b/N_0 was 20 dB, the GFDM/OQAM system obtained a BER performance of 0.16. On the other hand, the GFDM/QAM system obtained a BER performance of 0.18. It can be concluded that the performance of GFDM/OQAM on Rayleigh channel when the value of $\alpha = 1$ is better than GFDM/QAM.

G. POWER SPECTRAL DENSITY ANALYSIS

This section analyzes the signal spectrum parameters in the simulation of the two systems, as shown in Figure 11. Spectral density of a signal is the distribution of signal power in the frequency region. It is very significant for understanding filtering systems in wireless communication systems. Power spectral density (PSD) was used to evaluate the signal or noise at the filter output [7].

The FFT converts the signal into the frequency domain to observe the transmitted information signal PSD. Welch's method was used to observe PSD. The PSD curve for the GFDM system is shown in Figure 10. The GFDM/OQAM had smaller sidelobes and OOB emissions than GFDM/QAM. The attenuation value for GFDM/OQAM was about -7 dB below the GFDM/QAM signal. It happens because there is a half-time symbol delay between the quadrature and in-phase components of the subcarrier in OQAM systems. In addition, OQAM also minimizes ICI effects by reducing the distance between adjacent channels for each subcarrier

V. CONCLUSION

This study has succeeded in comparing the performance of the GFDM system with QAM and OQAM. It has also investigated the performance of both systems for BER parameters, constellation diagrams, and signal spectrum. The advantage of GFDM/OQAM over GFDM/QAM is that the quadrature and in-phase components of OQAM modulation do not shift in the same time slot. In addition, GFDM/OQAM had low OOB and high data rate; and was free from ICE. The roll-off factor value greatly affects the performance of the GFDM system. If the value of α is higher, so is the value of BER. This study succeeded in obtaining a reference value of roll-off factor that could be used in the application of the GFDM/OQAM system with the best performance result of 0.3. The next research is to investigate MIMO-GFDM using QAM and OQAM mapping on AWGN and Rayleigh channels.

CONFLICT OF INTEREST

The author declares that there is no conflict of interest.

AUTHOR CONTRIBUTION

Conceptualization, Ari Endang Jayati and Budiani Desyningtias; methodology, Ari Endang Jayati; software, first author; validation, Ari Endang Jayati, Budiani Desyningtias; formal analysis, Ari Endang Jayati; investigation, Ari Endang Jayati; resources, Ari Endang Jayati; data curation, Ari Endang Jayati; writing—original drafting, Ari Endang Jayati; writing—review and editing, Ari Endang Jayati; visualization, Ari Endang Jayati; supervision, Ari Endang Jayati; project administration, Ari Endang Jayati; funding acquisition, Budiani Desyningtias.

ACKNOWLEDGMENT

Our gratitude goes to LPPM Semarang University for funding this research.

REFERENCES

[1] N. Michailow *et al.*, "Generalized Frequency Division Multiplexing: A Flexible Multi-Carrier Modulation Scheme for 5th Generation Cellular Networks," *Proc. German Microwave Conference (GeMiC'12)*, 2012, pp. 1–4.

[2] S.K. Bandari, V.V. Mani, and A. Drosopoulos, "OQAM Implementation of GFDM," *2016 23rd Int. Conf. Telecommun. (ICT)*, 2016, pp. 1–5, doi: 10.1109/ICT.2016.7500463.

[3] S. Randel, *et al.*, "Study of Multicarrier Offset-QAM for Spectrally Efficient Coherent Optical Communications," *2011 37th Eur. Conf., Exhib. Opt. Commun.*, 2011, pp. 5–11.

[4] S.K. Bandari, V.V. Mani, and A. Drosopoulos, "GFDM/OQAM Implementation under Rician Fading Channel," *2016 Int. Conf. Adv. Comput., Commun., Inform. (ICACCI)*, 2016, pp. 256–260, doi: 10.1109/ICACCI.2016.7732056.

[5] I. Gaspar *et al.*, "Frequency-Shift Offset-QAM for GFDM," *IEEE Commun. Lett.*, Vol. 19, No. 8, pp. 1454–1457, Aug. 2015, doi: 10.1109/LCOMM.2015.2445334.

[6] A.E. Jayati, Wirawan, T. Suryani, and Endroyono, "Teknik Mitigasi Efek Nonlinieritas High Power Amplifier (HPA) pada Multiple Input Multiple Output (MIMO) Generalized Frequency Division Multiplexing (GFDM)," Dissertation, Institut Teknologi Sepuluh Nopember, Indonesia, 2021.

[7] A.E. Jayati, Wirawan, T. Suryani, and Endroyono. "Nonlinear Distortion Cancellation Using Predistorter in MIMO-GFDM Systems," *Electron.*, Vol. 8, No. 6, pp. 1–19, Jun. 2019, doi: 10.3390/electronics8060620.

[8] A.E. Jayati, Wirawan, Wirawan, and T. Suryani. "Analysis of Non-Linear Distortion Effect Based on Saleh Model in GFDM System*." 2017 IEEE Int. Conf. Commun. Netw., Satell. (Comnetsat)*, 2017, pp. 1–6, doi: 10.1109/COMNETSAT.2017.8263564.

[9] A.E. Jayati and B. Destyningtias, "The Analysis of the High Power Amplifier Distortion on the MIMO-GFDM System," *2021 IEEE Int. Conf. Commun. Netw., Satell. (COMNETSAT)*, 2021, pp. 252–257, doi: 10.1109/COMNETSAT53002.2021.9530796.

[10] F.H. Ramadiansyah, T. Suryani, and Suwadi, "Perbaikan Kinerja Sistem Generalized Frequency Division Multiplexing dengan Menggunakan Offset Quadrature Amplitude Modulation," Undergraduate thesis, Institut Teknologi Sepuluh Nopember, Surabaya, Indonesia, 2017.

[11] N. Michailow *et al.*, "Generalized Frequency Division Multiplexing for 5th Generation Cellular Networks," *IEEE Trans. Commun.*, Vol. 62, No. 9, pp. 3045–3061, Sep. 2014, doi: 10.1109/TCOMM.2014.2345566.

[12] S.K. Antapurkar, A. Pandey, and K.K. Gupta, "GFDM Performance in Terms of BER, PAPR and OOB and Comparison to OFDM System," *AIP Conf. Proc.*, Vol. 1715, No. 1, pp. 1–11, 2016, doi: 10.1063/1.4942721.

[13] S.S.K.C. Bulusu, H. Shaïek, and D. Roviras, "HPA Linearization for Next Generation Broadcasting Systems with Fast Convergence-Digital Predistortion," *IEEE Trans. Broadcast*., Vol. 67, No. 3, pp. 776–790, Sep. 2021, doi: 10.1109/TBC.2021.3081925.

[14] G. Qiao *et al*., "Low-Complexity Progressive MIMO-OFDM Receiver for Underwater Acoustic Communication," *Symmetry*, Vol. 11, No. 3, pp. 1–16, Mar. 2019, doi:10.3390/sym11030362.

[15] A. Mohammadian, A. Mohammadi, A. Abdipour, dan M. Baghani, "Spectral Analysis of GFDM Modulated Signal under Nonlinear Behavior of Power Amplifier," *Wirel. Netw.*, Vol. 27, pp. 137–149, Aug. 2021, doi: 10.1007/s11276-020-02403-2.

[16] Z.A. Sim *et al*., "Performance of GFDM Systems Using Quadratic Programming Pulse Shaping Filter Design," *IEEE Access*, Vol. 8, pp. 37134–37146, Feb. 2020, doi: 10.1109/ACCESS.2020.2975430.

[17] L.L. Mendes and H.D Rodrigues. "Inatel Prototypes GFDM Transceiver to Bring 5G to Brazilian Remote Areas in a Fraction of Time," IEEE Spectrum. https://spectrum.ieee.org/inatel-prototypes-gfdm-transceiver-to-bring-5g-to-brazilian-remote-areas-in-a-fraction-of-time, access date: 2-Jan-2021.

[18] V. Kumar, B. Cardiff, and M.F. Flanagan, "Performance Analysis of NOMA with Generalized Selection Combining Receivers," *Electron. Lett.*, Vol. 55, No. 25, pp. 1364–1367, Dec. 2019, doi: 10.1049/el.2019.2948.

[19] A.E. Jayati, Wirawan, T. Suryani, and Endroyono, "Characteristic of HPA Nonlinear Distortion Effects in MIMO-GFDM Systems," *2018 Int. Conf. Inf., Commun. Technol. Converg. (ICTC)*, 2018, pp. 379–384, doi: 10.1109/ICTC.2018.8539527.

[20] A.E. Jayati and M. Sipan, "Impact of Nonlinear Distortion with the Rapp Model on the GFDM System," *2020 Third Int. Conf. Vocat. Educ., Elect. Eng. (ICVEE)*, 2020, pp. 1–5, doi: 10.1109/ICVEE50212.2020.9243295.